



## Dynamics of domain walls governed by the convective Cahn–Hilliard equation

A. Podolny<sup>a</sup>, M.A. Zaks<sup>b</sup>, B.Y. Rubinstein<sup>c</sup>, A.A. Golovin<sup>d,\*</sup>, A.A. Nepomnyashchy<sup>a,d</sup>

<sup>a</sup> Department of Mathematics, Technion, Israel Institute of Technology, 32000 Haifa, Israel

<sup>b</sup> Institute of Physics, Humboldt University, D-12489 Berlin, Germany

<sup>c</sup> Department of Mathematics, University of California, Davis, CA 95616, USA

<sup>d</sup> Department of Engineering Sciences and Applied Mathematics, Northwestern University, Evanston, IL 60208, USA

Received 9 June 2004; received in revised form 2 January 2005; accepted 10 January 2005

Communicated by C.K.R.T. Jones

### Abstract

The convective Cahn–Hilliard (CCH) equation,  $u_t + (u_{xx} + u - u^3)_{xx} - (D/2)(u^2)_x = 0$ , has been suggested recently for the description of several physical phenomena, including spinodal decomposition of (driven) phase separating systems in an external field, instability of steps moving on a crystal surface, and faceting of growing, thermodynamically unstable surfaces. In this paper the dynamics of domain walls (kinks) governed by the convective Cahn–Hilliard equation is studied by means of asymptotic and numerical methods. A special attention is paid to the dynamics of kink pairs and triplets that play crucial role in the coarsening (Ostwald ripening) process. For the driving parameter  $D < D_0 = \sqrt{2}/3$  and large distance between the kinks,  $L \gg 1$ , analytical formulas are found that describe the motion of the kink pairs and triplets. The analytical formulas are in excellent agreement with the results of direct numerical simulations of CCH equation. They explain the logarithmically slow coarsening observed for the kink dynamics governed by CCH equation when the distances between the kinks become large, unlike the fast coarsening for moderate distances between the kinks at intermediate stages.

© 2005 Elsevier B.V. All rights reserved.

PACS: 64.75.+g; 89.75.Kd

Keywords: Cahn–Hilliard equation; Phase separation; Coarsening; Domain walls

### 1. Introduction

The dynamics of domain walls (named also kinks) between different broken-symmetry phases plays the crucial role in the transition from a disordered phase to an ordered phase [1] and in the development of the spatial chaos [2].

\* Corresponding author. Tel.: +1 847 4915346; fax: +1 847 4912178.

E-mail address: [a-golovin@northwestern.edu](mailto:a-golovin@northwestern.edu) (A.A. Golovin).

In potential systems, characterized by a monotonically decreasing Lyapunov (free energy) functional, the evolution leads to an equilibrium state with the minimum number of domain walls, since they have some excess free energy. The dynamics of domain walls is rather different in systems without and with a conservation law [3]. In systems without a conservation law, the typical dynamics is governed by the Allen–Cahn equation [1]. The domain walls move towards each other and annihilate, so that the characteristic length of the domains grow with time (coarsening). In systems with a conservation law, the evolution is typically described by the Cahn–Hilliard equation [1]. In this case, the mutual motion of domain walls is complicated by the conservation law, and the coarsening takes place through a collective motion of kink aggregates rather than individual kinks [3]. In the case of a (1D) Cahn–Hilliard equation, the interaction of kinks exponentially decays with the distance between them so that the coarsening rate is logarithmically slow [4].

If a system is not potential, the evolution does not generally lead to the state characterized by the minimum value of the free energy. Under some conditions the final state contains a finite number of defects, i.e. some ordered or disordered patterns are formed. The latter phenomenon takes place when the domain walls have oscillating tails [2]. In strongly non-potential systems, e.g. like those governed by the Kuramoto–Sivashinsky equation [5], the spatio-temporal chaos characterized by a spontaneous creation and annihilation of defects, is developed.

Recently, a non-potential modification of the Cahn–Hilliard equation, the *convective (or driven) Cahn–Hilliard equation* (CCH),

$$u_t + (u_{xx} + u - u^3)_{xx} - \frac{D}{2}(u^2)_x = 0, \quad (1)$$

was suggested for the description of several physical phenomena, namely spinodal decomposition of phase separating systems in an external field [6–8], step instability on a crystal surface [9], as well as faceting of growing, thermodynamically unstable surfaces under non-equilibrium conditions [10–15]. A similar equation describes also dewetting of a thin liquid film flowing down a slightly inclined plane [16,17]. The regular Cahn–Hilliard equation corresponds to the case  $D = 0$ , while the Kuramoto–Sivashinsky equation is obtained in the limit  $D \rightarrow \infty$  by the transformation  $u \rightarrow u/D$  [13]. It was found in [13] that the coarsening dynamics described by the convective Cahn–Hilliard equation is strongly influenced by the asymptotic behavior of kink tails. If  $D > D_0 = \sqrt{2}/3$ , the kinks have oscillating tails, that leads to the development of ordered or disordered, spatially non-uniform structures, in accordance with the arguments given in [2] (see also [9]). For  $D < D_0 = \sqrt{2}/3$ , the tails are monotonic, and the solutions of Eq. (1) exhibit coarsening governed by the interaction between the kinks and their collective motion.

When the characteristic distance between the kinks,  $L$ , is large, the kink dynamics can be studied analytically. Emmott and Bray [8] considered the limit  $DL \ll 1$  and suggested some model equations for the motion of kinks. They found that a pair of kinks (kink–antikink pair) performs a collective motion with a velocity determined by  $D$  and  $L$ , that leads to *fast* coarsening such that  $L \sim t^{1/2}$ . However, direct numerical solution of Eq. (1) performed in [13] showed that the fast coarsening regime exhibits the crossover to a logarithmically slow coarsening for sufficiently large  $L$ , which is typical of the standard Cahn–Hilliard equation. Watson et al. [14] explained this crossover for the case when  $D \ll 1$  and the product  $DL$  is arbitrary, and derived the equations of motion for kinks by means of the asymptotic analysis. The analysis presented in [14] revealed the important role of *kink triplets* where a negative kink (“antikink”) situated in the middle of the triplet attracts two positive kinks on its both sides, eventually leading to simultaneous annihilation of the triplet and the formation of a new positive kink.

In the present paper, we investigate the dynamics of kinks governed by the CCH equation for *arbitrary*  $0 < D < D_0$  in the case when the distances between the kinks are large,  $L \gg 1$ . The results of the asymptotic analysis are justified by numerical simulations. In Section 2, we discuss the individual kinks and show that the stable antikink is unique and motionless, while the moving kinks form a two-parameter family of solutions. Sections 3 and 4 are devoted to the consideration of pairs and triplets of kinks, respectively.

## 2. Constant solutions and kinks

We shall start the investigation of the kink dynamics governed by Eq. (1) with the consideration of its simplest solutions. Without loss of generality, we assume  $D > 0$ .

First, let us note that any constant  $u = U_0$  is a solution of Eq. (1). In order to study the linear stability of this solution, linearize Eq. (1),

$$u = U_0 + \tilde{u}(x) e^{\sigma_0 t},$$

and find the eigenfunctions and the eigenvalues:

$$\tilde{u}(x) = e^{ikx}, \quad \sigma_0(k) = (1 - 3U_0^2)k^2 - k^4 - ikDU_0. \tag{2}$$

Obviously, the constant solutions are linearly stable if

$$|U_0| > \frac{1}{\sqrt{3}}. \tag{3}$$

Let us consider now traveling wave solutions,

$$u = U(X), \quad X = x - vt, \quad v = \text{const}. \tag{4}$$

Substituting (4) into (1) and integrating once with respect to  $X$ , one obtains the following ordinary differential equation:

$$U_{XXX} + (U - U^3)_X - vU - \frac{D}{2}U^2 = -J, \quad -\infty < X < \infty, \tag{5}$$

where  $J$  is the integration constant. Eq. (5) has different kinds of solutions, e.g. periodic or quasiperiodic ones. Here we consider *heteroclinic* solutions (“domain walls” or “kinks”) that connect two critical points of the dynamical system (5):

$$U = U_{\pm} = -\frac{v}{D} \pm \sqrt{\left(\frac{v}{D}\right)^2 + \frac{2J}{D}}, \tag{6}$$

$J > -v^2/2D$ . Note that in the case  $v = 0$ ,  $U_- = -U_+$ . Depending on the boundary conditions, the heteroclinic solutions can be of two types:

*positive kinks*, with

$$U(\pm\infty) = U_{\pm}, \tag{7}$$

and *negative kinks*, or *antikinks*, with

$$U(\pm\infty) = U_{\mp}. \tag{8}$$

Later on, we shall consider only the case with  $|U_{\pm}| > 1/\sqrt{3}$ , i.e. when both constant solutions  $U = U_{\pm}$  are stable.

In order to investigate the asymptotics of the heteroclinic solutions at  $x \rightarrow \pm\infty$ , linearize Eq. (5) around the constant solutions,  $U = U_{\pm}$ ,

$$U(X) = U_{\pm} + \tilde{U} e^{\kappa X}, \tag{9}$$

to obtain the following equation for the eigenvalues  $\kappa$ :

$$\kappa^3 - (3U_{\pm}^2 - 1)\kappa - (v + DU_{\pm}) = 0. \tag{10}$$

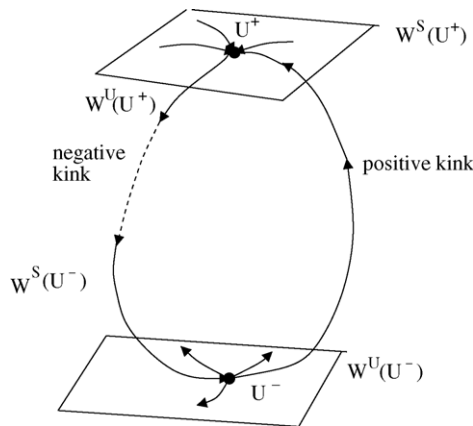


Fig. 1. A diagram of the stable and unstable manifolds of stationary points of Eq. (5) and heteroclinic solutions corresponding to positive and negative kinks.

Depending on the sign of  $Q = -[(3U_{\pm}^2 - 1)/3]^3 + [(v + DU_{\pm})/2]^2$ , two cases are possible: (i) for  $Q \leq 0$  all roots of Eq. (10),  $\kappa_j, j = 1,2,3$ , are real; (ii) for  $Q > 0$  one root is real and two other roots are complex conjugate. In the case (ii), the kinks have oscillatory tails, and one can expect the development of ordered or disordered structures rather than a system of kinks [2,13]. In the present paper we consider the case (i), when the system evolution is determined by the motion of kinks.

Since  $\kappa_1 + \kappa_2 + \kappa_3 = 0$ , the roots  $\kappa_j$  cannot have the same sign. Taking into account that

$$\kappa_1\kappa_2\kappa_3 = v + DU_{\pm} = \pm\sqrt{v^2 + 2DJ}$$

is positive for  $U = U_+$  and negative for  $U = U_-$ , one concludes that in the former case two eigenvalues are negative and one eigenvalue is positive, while in the latter case two eigenvalues are positive and one eigenvalue is negative. In other words, for the critical point  $U = U_+$  ( $U = U_-$ ) the unstable manifold  $W^u(U_+)$  (the stable manifold  $W^s(U_-)$ ) is one-dimensional, while the stable manifold  $W^s(U_+)$  (the unstable manifold  $W^u(U_-)$ ) is two-dimensional.

According to its definition, the kink corresponds to a trajectory on  $M_+ = W^u(U_-) \cap W^s(U_+)$ , while the antikink is situated on  $M_- = W^u(U_+) \cap W^s(U_-)$ , see Fig. 1. In the former case,  $M_+$  is an intersection of two two-dimensional manifolds in a three-dimensional space, which is generic and exists in a certain region in the parameter space  $(v, J)$ . A particular kink solution can be written explicitly,

$$U(X) = C \tanh \frac{C}{\sqrt{2}}(X - X_0), \quad C = \sqrt{1 + \frac{D}{\sqrt{2}}}, \quad X_0 = \text{const},$$

for  $v = 0, J = DC^2/2$ , but a two-parameter family of kinks exists for certain intervals of  $v$  and  $J$  values. For fixed values of  $U_-$  and  $U_+$ , the velocity of the kink is calculated to be

$$v = -\frac{D}{2}(U_- + U_+).$$

An antikink can exist only if the trajectory  $W^u(U_+)$  reaches the vicinity of the point  $U_-$  exactly along the trajectory  $W^s(U_-)$  (see Fig. 1). Such event has a codimension 2 in the parameter space. Therefore, one can expect that the

antikink exists for isolated values of  $(v, J)$ . Indeed, there exists a solution<sup>1</sup>

$$U = -A \tanh \frac{A}{\sqrt{2}}(X - X_0), \quad A = \sqrt{1 - \frac{D}{\sqrt{2}}}, \quad X_0 = \text{const}, \tag{11}$$

for  $v = 0, J = DA^2/2$ .

Note that for  $v = 0, U_{\pm} = \pm A$  the roots of the cubic equation (10) are described by simple formulas,

$$\kappa_1 = \mp \frac{A + B}{\sqrt{2}}, \quad \kappa_2 = \mp \frac{A - B}{\sqrt{2}}, \quad \kappa_3 = \pm A\sqrt{2}, \tag{12}$$

where  $A$  is defined by Eq. (11), and

$$B = \sqrt{1 - \frac{3D}{\sqrt{2}}}. \tag{13}$$

All three roots are real if  $D < D_0 = \sqrt{2}/3$ .

### 3. Antikink–kink pairs

Let us consider now the interaction of distant kinks. Since this interaction is expected to decrease exponentially with the distance between the kinks [14], the dynamics is typically determined by the pair of the closest kinks, while the motion of other kinks is negligible compared with the motion of this pair. In the present section, we consider a kink pair described by a *homoclinic solution*,<sup>2</sup>  $U = U_h(X)$  ( $X = x - vt, v = \text{const}$ ), of the dynamic system (5), that satisfies the boundary condition

$$U(-\infty) = U(+\infty) = U_+. \tag{14}$$

Note that if  $U = U_h(X)$  is a solution of Eq. (5), then  $U = -U_h(-X)$  is also a solution. Therefore, it is sufficient to consider the case  $U_+ > 0$  (i.e. the case when the antikink is located to the left from the kink). Numerical solution of Eq. (1) in the form of such antikink–kink pair at a particular moment of time is shown in Fig. 2a. The solution has been performed by means of a pseudospectral code, with time integration in Fourier space using the Crank–Nicolson scheme for the linear operator and Adams–Bashford scheme for the nonlinear operator, with periodic boundary conditions and the initial conditions close to the antikink–kink pair. Note that the antikink–kink pair presented in Fig. 2a is moving slowly to the left with a constant speed, as shown in Fig. 2b (see below).

The homoclinic trajectory  $U_h(X)$  corresponds to the trajectory  $W^u(U_+)$  that has to return to the point  $U_+$  along its two-dimensional stable manifold (see Fig. 1). This is a codimension 1 event, therefore in the two-dimensional parameter space  $(v, J)$  the homoclinic trajectories should exist on a curve (or on a set of curves). Thus, antikink–kink pairs form a *one-parameter* family, and the velocity of a pair  $v$  may be viewed a function of  $J$ .

We shall use a more physically meaningful parametrization of kink–antikink pairs, taking as the basic parameters the *distance*  $L$  between the kink centers, i.e. between the points where  $U(X) = 0$ . In this case, both parameters  $v$  and  $J$  have to be calculated as functions of  $L$ .

<sup>1</sup> The numerical investigation of Eq. (5) reveals the existence of other isolated heteroclinic ( $U_+ \rightarrow U_-$ ) solutions with  $v = 0, J < DA^2/2$ , which correspond to non-monotonic functions  $U(X)$ . These solutions have never been observed in the simulations of the original problem (1), and they are apparently unstable.

<sup>2</sup> Actually, the dynamic system (5) has many homoclinic solutions. Here we discuss a specific family of homoclinic solutions that correspond to antikink–kink pairs.

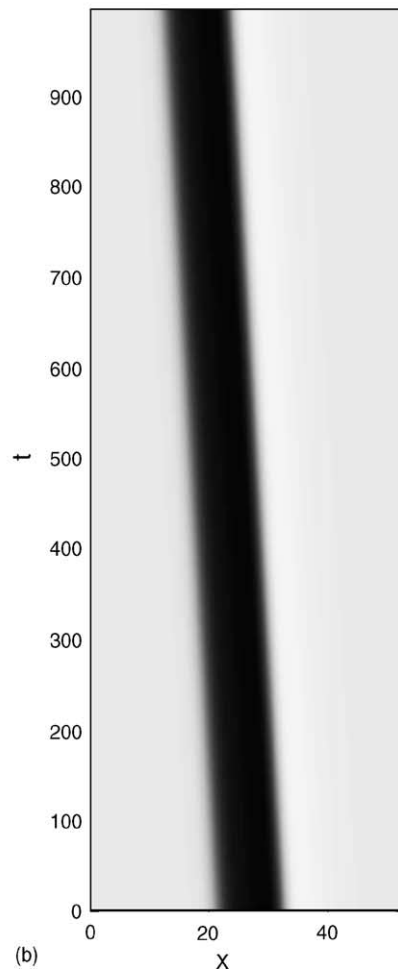
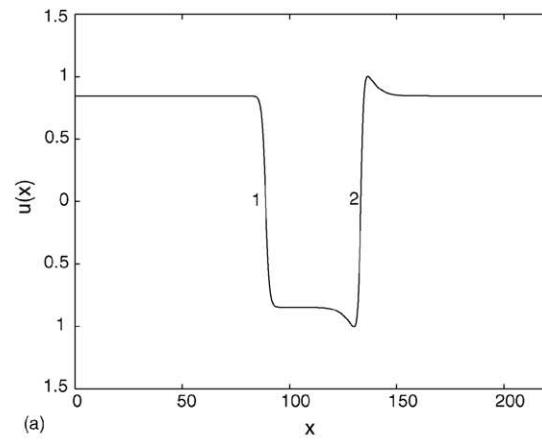


Fig. 2. (a) Numerical solution of Eq. (1) in the form of an antikink–kink pair (1, antikink; 2, kink), very slowly moving to the left with a constant speed;  $D = 0.4$ . (b) Space-time diagram showing numerical solution of Eq. (1) in the form of a uniformly moving antikink–kink pair (the distance between the kinks is less than that shown in (a)).

In order to find these functions in the limit of large  $L$ , we shall use the approach similar to that applied in [18] for the analysis of the interaction between solitons and in [3] for the analysis of the interaction between kinks governed by the Allen–Cahn equation and by standard Cahn–Hilliard equation. We shall construct the solution of the *nonlinear* equation (5) as a *linear superposition* of two kink solutions with a certain correction, which is caused by the nonlinearity and has to be calculated. The solvability conditions for that correction determine the parameters  $v$  and  $J$  (see below).

We expect that at large  $L$  the velocity of a kink pair is small, and for the slowly moving pair containing an antikink,  $U(-\infty) = U_+$  will be close to  $A = \sqrt{1 - D/\sqrt{2}}$  that corresponds to a sole motionless antikink (11). In order to match the condition  $U(+\infty) = U_+$ , one has to take a kink with the parameter  $U_+$  close to  $A$  as well. Thus, one can construct a solution as [3,18],

$$U(X) = U_1(X) + U_2(X) + A + \tilde{u}(X), \tag{15}$$

where  $U_1(X)$  is the negative kink described by (11) with  $X_0 = 0$ , and  $U_2(X)$  is a representative of the family of kinks corresponding to  $v = 0$ ,  $J = DA^2/2$ , with the center located in the point  $X = L$ , and  $\tilde{u}(X)$  is a small correction that includes the difference between  $U_+$  for a kink pair and  $A$  selected by the motionless negative kink. Unlike the antikink, the kink cannot be presented in an analytical form. Note that the asymptotics of the kink solution for large negative  $X - L$  is determined by the eigenvalues (12) calculated near the critical point  $U = -A$ . The left “tail” of the kink is characterized by the smallest positive eigenvalue,  $\kappa_2 = (A - B)/\sqrt{2}$ , and can be written as

$$U_2(X) + A = u_2(X) \sim a(D) \exp[\kappa_2(X - L)], \tag{16}$$

where the constant  $a(D)$  can be calculated analytically only in the limit of small  $D$ . Using the matched asymptotic expansions, one finds that for  $D \ll 1$

$$a(D) \sim -D\sqrt{2}/2, \tag{17}$$

(see [14]). In the general case, the constant  $a(D)$  is found numerically to be negative (see also [8]). The numerically computed function  $a(D)$  is shown in Fig. 3.

It is convenient to rewrite Eq. (5) in the form

$$U_{XXX} + (U - U^3)_X - \frac{D}{2}(U^2 - A^2) = q + vU, \quad -\infty < X < \infty, \tag{18}$$

where  $q = -J + DA^2/2$ , which is zero for individual kinks, is expected to be small for a kink pair.

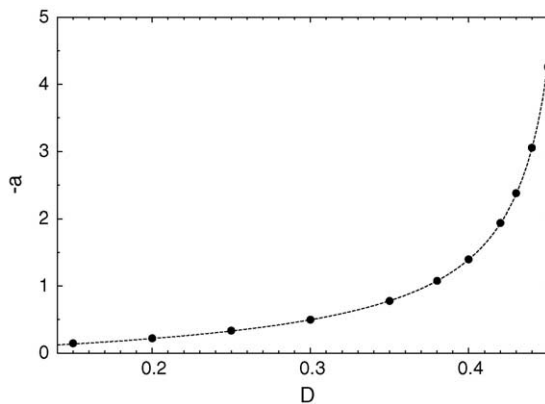


Fig. 3. The function  $a(D)$  found from numerical data.

Substitute (15) into Eq. (18) and linearize the latter with respect to  $\tilde{u}$ . According to the approach of [3,18], we separately consider the regions around the centers of the left and the right kinks.

Near the left kink ( $X = O(1)$ ) the contribution of the right kink,  $U_2(X)$ , is exponentially small. We can replace the function  $U_2(X) + A$  by its asymptotic limit  $u_2(X)$  and linearize Eq. (19) also with respect to  $u_2$ . Taking into account that  $u_2(X)$  satisfies the equation:

$$u_{2XXX} + (1 - 3A^2)u_{2X} - DAu_2 = 0,$$

we obtain the following equation for  $\tilde{u}(X)$  valid in the region  $X = O(1)$ :

$$\tilde{u}_{XXX} + [(1 - 3U_1^2)\tilde{u}]_X - DU_1\tilde{u} = q + vU_1 + [3(U_1^2 - A^2)u_2]_X + D(U_1 + A)u_2. \tag{19}$$

Recall that the functions  $U_1(X)$  and  $U_2(X)$  are determined by the formulas (11) with  $X_0 = 0$ , and (16), respectively.

The solution of Eq. (19) is bounded if its right-hand side is orthogonal to two bounded solutions of the adjoint problem,

$$u_{XXX}^c + (1 - 3U_1^2)u_X^c + DU_1u^c = 0, \tag{20}$$

that can be found analytically:

$$u_-^c(X) = \frac{\sinh(BX/\sqrt{2})}{\cosh(AX/\sqrt{2})} \tag{21}$$

is an odd function, and

$$u_+^c(X) = \frac{\cosh(BX/\sqrt{2})}{\cosh(AX/\sqrt{2})} \tag{22}$$

is an even function.<sup>3</sup> Taking into account that  $U_1(X)$  is an odd function, we obtain two equations that determine  $v$  and  $q$  as functions of  $L$  and  $D$ :

$$v \int_{-\infty}^{+\infty} dXu_-^c U_1 + 3 \int_{-\infty}^{+\infty} dXu_-^c [(U_1^2 - A^2)u_2]_X + D \int_{-\infty}^{+\infty} dXu_-^c (U_1 + A)u_2 = 0, \tag{23}$$

$$q \int_{-\infty}^{+\infty} dXu_+^c + 3 \int_{-\infty}^{+\infty} dXu_+^c [(U_1^2 - A^2)u_2]_X + D \int_{-\infty}^{+\infty} dXu_+^c (U_1 + A)u_2 = 0. \tag{24}$$

The integrals in (23) and (24) can be calculated analytically. For example, the explicit formula for the velocity of an antikink–kink pair,  $v \equiv v_2(D, L)$ , can be written as

$$v_2(D, L) = a(D)C_2(D) e^{-\kappa_2 L}, \tag{25}$$

where

$$C_2(D) = \frac{\cos(\beta\pi/2)[D\sqrt{2} + A^2(3\beta - 1)]}{\sqrt{2}\beta\pi}, \tag{26}$$

and

$$\beta = \frac{B}{A} = \sqrt{\frac{\sqrt{2} - 3D}{\sqrt{2} - D}}. \tag{27}$$

<sup>3</sup> The third linearly independent solution of Eq. (20),  $u_0^c(X) = 1 + D/3(\sqrt{2} - D) \cosh^2(AX/\sqrt{2})$ , is unbounded and not relevant.



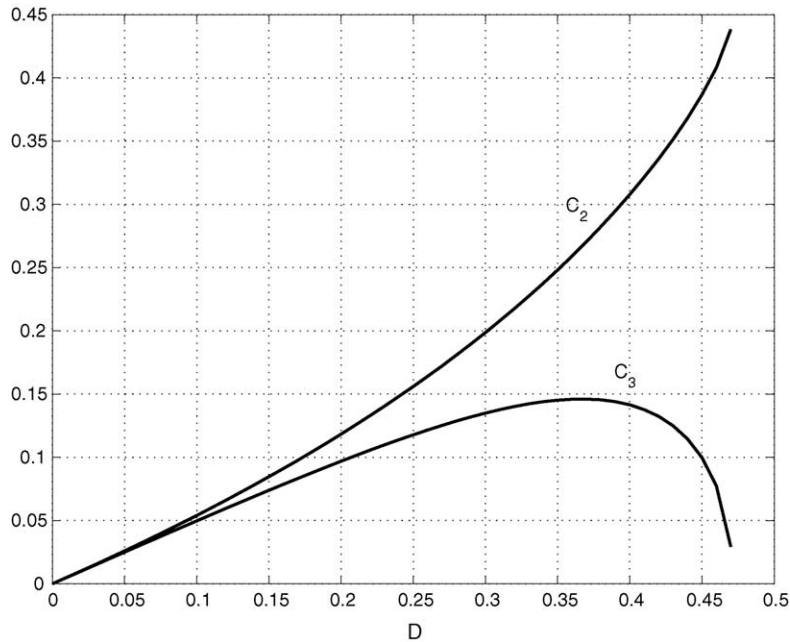


Fig. 4. Dependences of the coefficients  $C_2$  and  $C_3$  on  $D$  (see formulas (25) and (39)).

The coefficient  $C_2(D)$  is positive for any values of  $D$  (see Fig. 4). In the limit  $D \rightarrow 0$ ,  $C_2(D) \sim D/2 + O(D^2)$ . Using the relation (17) and taking into account that  $\kappa_2 \sim D/2$ , one finds that in the limit  $D \ll 1$ ,  $DL \gg 1$ ,

$$v_2(D, L) \sim - \left( \frac{D^2 \sqrt{2}}{4} \right) \exp \left( - \frac{DL}{2} \right),$$

that coincides with the result of Watson et al. [14]. In the limit  $D \rightarrow D_0 = \sqrt{2}/3$ ,  $C_2(D) \sim \sqrt{2}/\pi - (D_0 - D)^{1/2} 2^{-1/4} \pi + O(D_0 - D)$ . As mentioned above, the constant  $a(D)$  in Eq. (28) cannot generally be found analytically for an arbitrary  $D$  and has to be found numerically. We have found that  $a(D) < 0$  for any  $D < D_0$ , and therefore  $v < 0$ , i.e. the antikink–kink pair moves to the left (i.e. the antikink is leading). Similarly, using the transformation  $U \rightarrow -U$ ,  $X \rightarrow -X$ , one can show that the kink–antikink pair moves with the same velocity to the right (hence again the antikink is leading).

We have verified Eq. (25) by comparing it with the results of numerical computations: (i) computation of a heteroclinic solution of the ODE (18); and (ii) direct numerical simulation of the motion of an antikink–kink pair by solving the original PDE (1) by means of the pseudospectral code described above. In both cases, we obtained identical results. Fig. 5 shows the comparison between analytical (solid lines) and numerical (stars) values of the pair velocity calculated for various values of  $D$ . A space-time diagram showing a moving antikink–kink pair is presented in Fig. 2b.

Near the center of the right (positive) kink, one obtains the following equation:

$$\tilde{u}_{XXX} + [(1 - 3U_2^2)\tilde{u}]_X - DU_2\tilde{u} = q + vU_2 + [3(U_2^2 - A^2)u_1]_X + D(U_2 + A)u_1, \tag{28}$$

where  $U_2(X)$  is the full solution corresponding to the kink, while  $u_1(X)$  is the exponential tail of the solution  $U_1(X)$  at large  $X$ . It is interesting that Eq. (28) provides no additional solvability conditions. The corresponding adjoint

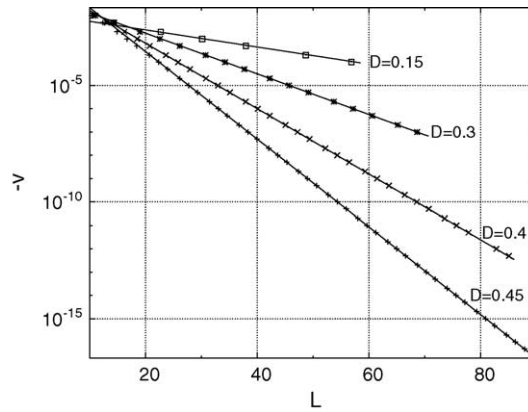


Fig. 5. Comparison between the velocity of an antikink–kink pair computed by Eq. (25) (solid lines) and the velocity obtained from numerical solution of Eq. (1) (squares, stars and crosses) for various values of  $D$ .

problem,

$$u_{XXX}^c + (1 - 3U_2^2)u_X^c + DU_2u^c = 0, \tag{29}$$

has no bounded solutions. Indeed, in the limit  $X - L \rightarrow +\infty$  the solution can be written as

$$u^c(X) = a_1 e^{k_1 X} + a_2 e^{k_2 X} + a_3 e^{k_3 X},$$

where  $k_{1,2,3}$  are the roots of the following characteristic equation:

$$k^3 + (1 - 3A^2)k + DA = 0. \tag{30}$$

Eq. (30) has two positive roots,  $k_1$  and  $k_2$ , and one negative root,  $k_3$ . Thus, the bounded solution has to satisfy two conditions,  $a_1 = 0$  and  $a_2 = 0$ . However, if  $u^c(X)$  is even with respect to  $X - L$ , i.e., generally,  $u^c(L) \neq 0$ ,  $u_{XX}^c(L) \neq 0$ , while  $u_X^c(L) = 0$ , one has only one fitting parameter,  $u_{XX}^c(L)/u^c(L)$  (note that Eq. (29) is linear) which is not sufficient to satisfy the two conditions. If  $u_c$  is odd then  $u^c(L) = u_{XX}^c(L) = 0$ ,  $u_X^c \neq 0$ , and the solution is unique up to a constant factor; therefore, one has no fitting parameters at all. Thus, generally, Eq. (29) has no bounded solutions.

The above-mentioned asymmetry between positive and negative kinks, caused by the differences in the manifold dimensions at infinity, and by the different dimensions of the solutions families, is rather unusual for problems of the interaction of spatially localized objects. We are not aware of any other similar examples.

#### 4. Kink triplets

In a multikink solution, the motion of a pair of neighboring kinks can be considered isolated until it approaches the kink to the left (to the right) of the antikink–kink (kink–antikink) pair. In both cases a configuration appears such that the antikink is located between the two kinks. Numerical solution of Eq. (1) in the form of a kink triplet at a particular moment of time is shown in Fig. 6a. The solution has been performed by the same pseudospectral code in a large domain with periodic boundary conditions and the initial condition close to the kink triplet in the center and an antikink near the boundary. In Fig. 6a only the central part of the domain with the kink triplet is shown. Since the domain is large, the antikink at the boundary does not affect the behavior of the kink triplet in the center. Because of the exponentially decaying interaction law, the influence of the third kink becomes significant when the distances  $L$

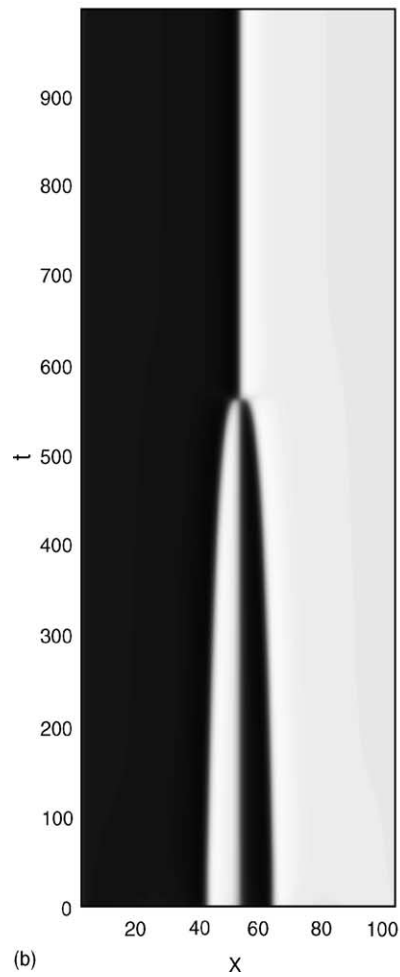
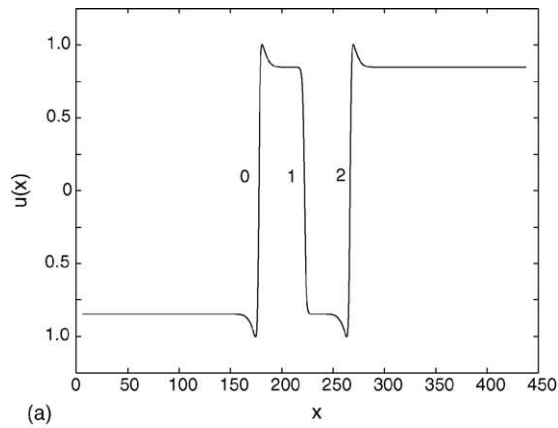


Fig. 6. (a) Numerical solution of Eq. (1) in the form of a symmetric kink triplet: 0.2, kinks; 1, antikink. The two kinks are moving with a small, constant speed towards the central, motionless antikink;  $D = 0.4$ . (b) Space-time diagram showing numerical solution of Eq. (1) in the form of a symmetric kink triplet in which the two kinks move towards the central antikink and annihilate (the distance between the kinks is less than that shown in (a)).

and  $L + \Delta L$  between the adjacent kinks are relatively small,  $\Delta L = O(1) \ll L$ . For the sake of simplicity, later on we shall consider a symmetric system of kinks where the central antikink (kink # 1) is located near the point  $x = 0$  while the two adjacent kinks are located at the points  $x = \mp L(t)$  (kinks # 0 and # 2). We are interested in finding the instantaneous velocity of the kink # 2,  $v_3(L) = dL/dt$ . Due to the symmetry of the system, the kink # 0 moves with the velocity  $-v_3$ , and the kink # 1 does not move at all.

Similar to (15), in the vicinity of the central kink the solution is represented as an odd function

$$u = U_1 + U_0 + U_2 + \tilde{u} \approx -A \tanh \frac{A}{\sqrt{2}}x - a(D)e^{-\kappa_2(x+L)} + a(D)e^{\kappa_2(x-L)} + \tilde{u}, \quad (31)$$

where  $\tilde{u}(x)$  describes the distortion of the central kink, decaying at large  $|x|$ . Since the terms  $\tilde{U}(x) = U_0(x) + U_2(x) + \tilde{u}(x)$  are small, one can linearize Eq. (1):

$$\tilde{U}_t + [\tilde{U}_{xx} + (1 - 3U_1^2)\tilde{U}]_{xx} - D(U_1\tilde{U})_x = 0. \quad (32)$$

Since the velocity of the kinks is assumed to be exponentially small, one can omit the term with the time derivative in the leading order and to integrate Eq. (32):

$$\tilde{U}_{xxx} + [(1 - 3U_1^2)\tilde{U}]_x - DU_1\tilde{U} = q, \quad (33)$$

where the constant  $q$  is to be found from the condition of solvability of Eq. (33) in the class of odd functions growing as  $\exp(\kappa_2|x|)$  (but not faster) at infinity.

Eq. (33) with  $U_1(x) = -A \tanh(Ax/\sqrt{2})$  is solved analytically. The general odd solution can be presented as the sum of the general odd solution of the homogeneous equation,<sup>4</sup>

$$\tilde{U}_h = C \cosh z [3 \cosh(\beta z)(A^2 \tanh^2 z - 1) \tanh z + \beta \sinh(\beta z)(1 + 2A^2 - 3A^2 \tanh^2 z)], \quad (34)$$

where  $z = Ax/\sqrt{2}$  and  $C$  is an arbitrary constant, and the partial solution of the inhomogeneous problem,

$$\tilde{U}_{ih}(z) = qF(z), \quad (35)$$

where  $F(z) = w(z)/\cosh^2 z$  and  $w(z)$  can be found in explicit form in terms of hypergeometric and algebraic functions of a new variable,  $\xi = \tanh z$ . For arbitrary  $C$  and  $Q$ , the asymptotic expression for the solution  $\tilde{U}(x)$  at large  $x$  contains two exponentially growing terms,

$$\tilde{U}(x) \sim a_1 \exp(\kappa_1 x) + a_2 \exp(\kappa_2 x),$$

where  $\kappa_1 = (A + B)/\sqrt{2}$ ,  $\kappa_2 = (A - B)/\sqrt{2}$ . For a solution representing the kink tails,  $a_1 \sim e^{-\kappa_1 L}$ ,  $a_2 \sim e^{-\kappa_2 L}$ ,  $a_1 \ll a_2$ , and therefore the coefficient  $a_1$  can be neglected in the leading order. This condition determines the relation between  $C$  and  $Q$  and the final expression for  $\tilde{U}(x)$ .

For large  $x$ , the obtained solution  $\tilde{U}(x)$  has the following asymptotics:

$$\tilde{U}(x) \sim q e^{\kappa_2 x} \frac{\sqrt{2}\pi[A^2(3 + \beta^2) - 5 + \beta^2]}{A^5 \beta(3 - \beta)(9 - \beta^2)(1 - \beta^2) \cos(\pi\beta/2)}. \quad (36)$$

Matching (36) with the known asymptotics of the kink tail,

$$\tilde{U}(x) \sim a(D)e^{-\kappa_2 L} e^{\kappa_2 x},$$

<sup>4</sup> The linearly independent even solutions of the homogeneous problem are  $\tilde{U}_1 = \cosh^{-2} z$  and  $\tilde{U}_2 = \cosh z [3 \sinh(\beta z)(A^2 \tanh^2 z - 1) \tanh z + \beta \cosh(\beta z)(1 + 2A^2 - 3A^2 \tanh^2 z)]$ . Note that only one solution of the linearized problem,  $\tilde{U}_1$ , is bounded as  $z \rightarrow \pm\infty$ , while the adjoint problem (20) has two bounded solutions, (21) and (22).

one finds

$$q = a(D)e^{-\kappa_2 L} \frac{A^5 \beta(3 - \beta)(9 - \beta^2)(1 - \beta^2) \cos(\pi\beta/2)}{\sqrt{2\pi}[A^2(3 + \beta^2) - 5 + \beta^2]}. \tag{37}$$

The velocity of the kinks can now be found from the conservation of flux (see [14]). Indeed, Eq. (1) can be written as

$$u_t + Q_x = 0, \tag{38}$$

where

$$Q = u_{xxx} + (u - u^3)_x - \frac{Du^2}{2}.$$

For a kink moving with the velocity  $v$ ,  $u = u(X)$ ,  $X = x - vt$ , Eq. (38) gives the conservation of the quantity  $Q - vu$ . Consider the kink # 2. Obviously, to the left of the kink center  $Q = -DA^2/2 + q$  and  $vu = -vA$  in the leading order. The velocity of the kink actually depends on the condition for the flux at infinity. If one assumes that the flux at infinity is  $Q = -DA^2/2$  and  $vu = vA$  (which corresponds to matching the kink amplitude to the next remote antikink), the conservation law gives

$$-\frac{DA^2}{2} + q + vA = -\frac{DA^2}{2} - vA,$$

therefore,  $v = -q/(2A)$ . Using (37), one finds the following expression for the velocity  $v \equiv v_3(D, L)$  of the right kink in the triplet (the left kink has the opposite velocity):

$$v_3(D, L) = a(D)C_3(D)e^{-\kappa_2 L}, \tag{39}$$

where

$$C_3(D) = \frac{A^4 \beta(3 - \beta)(9 - \beta^2)(1 - \beta^2) \cos(\pi\beta/2)}{2\pi\sqrt{2}[5 - \beta^2 - A^2(3 + \beta^2)]}, \tag{40}$$

$\beta$  is defined in (27) and  $a(D)$  is the same as in Eq. (25) for the velocity of an antikink–kink pair. The dependence  $C_3(D)$  is shown in Fig. 4. In the limit  $D \rightarrow 0$ ,  $C_3(D) \sim D/2 + O(D^2)$ , and we reproduce the result of Watson et al. [14]:

$$v_3(D, L) \sim v_2(D, L) \sim -(D^2\sqrt{2}/4) \exp(-DL/2),$$

for  $D \ll 1$ ,  $DL \gg 1$ . In the limit  $D \rightarrow D_0$ ,  $C_3(D) \sim 3(D_0 - D)^{1/2}2^{-1/4}\pi + O(D_0 - D)$ . The sign of  $v_3(D, L)$  is negative, that corresponds to the attraction of the positive kinks to the central negative kink. The comparison between the analytical formula (39) and the results of the numerical solution of Eq. (1) for various values of  $D$  is presented in Fig. 7.

The attraction of two kinks to the central antikink leads to their annihilation and to the transformation of the triplet into a new kink. The space-time diagram showing the motion and annihilation of two kinks in a triplet, obtained by the numerical solution of Eq. (1), is presented in Fig. 6b. The annihilation stage cannot be studied by means of the asymptotic theory.

For  $D > D_0$ , the kinks have oscillatory tails, and stable stationary patterns are formed instead of kinks (see [13]). Thus, we do not consider the kink dynamics in this region.

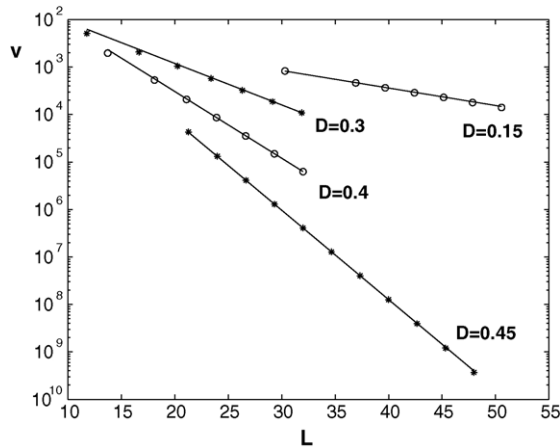


Fig. 7. Comparison between the velocity of a kink–antikink–kink triplet computed by Eqs. (39) and (40) (solid lines) and the velocity obtained from numerical solution of Eq. (1) (stars and circles), for various values of  $D$ .

## 5. Conclusions

We have studied the interaction and motion of domain walls (kinks) governed by a convective Cahn–Hilliard equation (1) that describes phase separation in driven systems. We have considered the case when the driving parameter,  $D$ , characterizing the external field or a driving force, can take any value below the critical one,  $D < D_0 = \sqrt{2}/3$ , above which the kinks have oscillatory tails and the coarsening stops [13]. We have shown that the stable negative kink (“antikink”) is unique while the positive kinks form a two-parameter family. With the driving parameter below this critical value and for the case when the distance between the two adjacent kinks,  $L$ , is large,  $L \gg 1$ , we have derived asymptotic formulas for the interaction between the kinks. We have shown that a kink–antikink pair moves in the direction of the antikink with a constant velocity which is a function of  $L$  and the driving parameter  $D$ . We have also shown that, as a result of this motion, kink–antikink–kink triplets are formed in which the two kinks move with the same speed towards the central antikink, finally annihilating and forming a single, larger kink. This process is the main mechanism of coarsening in a driven phase separating system described by the convective Cahn–Hilliard equation, not only for small driving force,  $D \ll 1$  [14], but for any  $D < D_0 = \sqrt{2}/3$ . Asymptotic formulas derived for the speed of the kink motion are in excellent agreement with the results of direct numerical simulation of Eq. (1). We have shown that, for any  $D < D_0$  the characteristic speed decreases exponentially with the distance between the kinks. This explains the crossover from the fast coarsening regime to the logarithmically slow one, that was observed in numerical simulations of the CCH equation [13] and in asymptotic analysis for the small driving force,  $D \ll 1$  [14]. Note that the dependence of the kink speed on the distance between the kinks in CCH equation is different from the case of the standard Cahn–Hilliard equation (Eq. (1) with  $D = 0$ ) where the characteristic kink speed decreases as  $L^{-1} \exp(-\text{const} \cdot L)$ . Our results show that in any quasi-one-dimensional, driven phase-separating system, with the driving force less than critical,  $D < D_0$ , the rate of the domain coarsening at sufficiently late stages, when  $L \gg 1$ , will be logarithmically slow.

## Acknowledgements

The authors are grateful to B. Matkowsky and D. Pelinovsky for useful discussion. A.A.N. acknowledges the hospitality of the ESAM Department of the Northwestern University and the support by the Eshbach Society. A.A.N. acknowledges also the support by the Minerva Center for Nonlinear Physics of Complex Systems funded through

the BMBF. A.A.G. acknowledges the support of the NIRT Program of the US National Science Foundation, grant DMR-0102794, and of the US Department of Energy, grant DE-FG02-03ER46069. M.Z. acknowledges the support of SFB-555.

## References

- [1] A.J. Bray, Theory of phase ordering kinetics, *Adv. Phys.* 43 (1994) 357.
- [2] P. Couillet, C. Elphick, D. Repaux, Nature of spatial chaos, *Phys. Rev. Lett.* 58 (1987) 431.
- [3] K. Kawasaki, T. Ohta, Kink dynamics in one-dimensional nonlinear systems, *Physica A* 116 (1982) 573.
- [4] T. Kawakatsu, T. Munakata, Kink dynamics in a one-dimensional conserved TDGL system, *Prog. Theor. Phys.* 74 (1985) 11.
- [5] T. Bohr, M.H. Jensen, G. Paladin, A. Vulpiani, *Dynamical System Approach to Turbulence*, University Press, Cambridge, 1998.
- [6] K. Leung, Theory of morphological instability in driven systems, *J. Stat. Phys.* 61 (1990) 345.
- [7] C. Yeung, T. Rogers, A. Hernandez-Machado, D. Jasnow, Phase-separation dynamics in driven diffusive systems, *J. Stat. Phys.* 66 (1992) 1071.
- [8] C.L. Emmott, A.J. Bray, Coarsening dynamics of a one-dimensional driven Cahn–Hilliard system, *Phys. Rev. E* 54 (1996) 4568.
- [9] Y. Saito, M. Uwaha, Anisotropy effect on step morphology described by Kuramoto–Sivashinsky equation, *J. Phys. Soc. Jpn.* 65 (1996) 3576.
- [10] F. Liu, H. Metiu, Dynamics of phase separation of crystal surfaces, *Phys. Rev. B* 48 (1993) 5808.
- [11] A.A. Golovin, S.H. Davis, A.A. Nepomnyashchy, A convective Cahn–Hilliard model for the formation of facets and corners in crystal growth, *Physica D* 122 (1998) 202.
- [12] A.A. Golovin, S.H. Davis, A.A. Nepomnyashchy, Model for faceting in a kinetically controlled crystal growth, *Phys. Rev. E* 59 (1999) 803.
- [13] A.A. Golovin, A.A. Nepomnyashchy, S.H. Davis, M.A. Zaks, Convective Cahn–Hilliard models: from coarsening to roughening, *Phys. Rev. Lett.* 86 (2001) 1550.
- [14] S.J. Watson, F. Otto, B.Y. Rubinstein, S.H. Davis, Coarsening dynamics of the convective Cahn–Hilliard equation, *Physica D* 178 (2003) 127.
- [15] M.E. Gurtin, *Thermomechanics of Evolving Phase Boundaries in the Plane*, Clarendon Press, Oxford, 1993.
- [16] U. Thiele, E. Knobloch, Front and back instability of a liquid film on a slightly inclined plate, *Phys. Fluids* 15 (2003) 892.
- [17] U. Thiele, E. Knobloch, Thin liquid films on a slightly inclined heated plate, *Physica D* 190 (2004) 213.
- [18] K.A. Gorshkov, L.A. Ostrovsky, Interaction of solitons in non-integrable systems: direct perturbation method and applications, *Physica D* 3 (1981) 428.